XXIst Moriond Astrophysics Meeting - Les Arcs March 10-17, 2001

DISCOVERY OF A CLUSTER OF GALAXIES (XMMU J183225.4-103645) TOWARDS GALACTIC PLANE WITH XMM-NEWTON

J. NEVALAINEN[1], D. LUMB[1], S. DOS SANTOS[2], H. SIDDIQUI[1], G. STEWART[2] & A. PARMAR[1]
[1] *Astrophysics Division, Space Science Department of ESA, ESTEC, Postbus 299, NL-2200 AG Noordwijk, The Netherlands*
[2] *Department of Physics and Astronomy, University of Leicester, University Road, Leicester LE1 7RH, UK*

During an XMM-Newton observation of the galactic supernova remnant G21.5-09 a bright, previously uncatalogued, source (XMMU J183225.4-103645) was detected 18′ from G21.5-09. The European Photon Imaging Camera data inside 1′ (180 h_{50}^{-1} kpc) radius are consistent with a source at a redshift of $0.1242\pm^{0.0003}_{0.0022}$ with an optically thin thermal spectrum of temperature 5.8 ± 0.6 keV and a metal abundance of 0.60 ± 0.10 solar. This model gives a 2 – 10 keV luminosity of $3.5^{+0.8}_{-0.4}$ h_{50}^{-2} 10^{44} erg s^{-1}. These characteristics, as well as the source extent of 2' (350 h_{50}^{-1} kpc), and the surface brightness profile are consistent with emission from the central region of a moderately rich cluster containing a cooling flow with mass flow rate of $\sim 400 - 600$ $M_\odot$ yr^{-1}. The absorption is (7.9 ± 0.5) 10^{22} atom cm^{-2}, 5 times that inferred from low-resolution HI data but consistent with higher spatial resolution infrared dust extinction estimates. XMMU J183225.4-103645 is not visible in earlier ROSAT observations due to high amount of absorption. This discovery demonstrates the capability of XMM-Newton to map the cluster distribution close to the Galactic plane, where few such systems are known. The ability of XMM-Newton to determine cluster redshifts to 1% precision at $z = 0.1$ is especially important in optically crowded and absorbed fields such as close to the Galactic plane, where the optical redshift measurements of galaxies are difficult.

1 Introduction

The clusters of galaxies trace the deepest gravitational potential wells, and their X-ray emission, which traces out the hot phase of inter-galactic gas, is less dependent on foreground contamination effects than optical cluster identification techniques. In addition, optical searches for clusters of galaxies have historically been forced to avoid a wide band of sky centered on the Galactic plane. The obscuration of ∼25% of the whole sky by the Galactic plane is problematic for the understanding of the dynamics in the local Universe, where the whole-sky map of the large scale structure is essential (Kraan-Korteweg & Lahav [6]).

With X-ray searches, the limiting factor is no longer extinction due to dust and confusion from stellar sources, but the amount of photo-electric absorption, N_H. The N_H and visual extinction rise roughly proportionally towards the Galactic plane, but because XMM-Newton has a lot of effective area above energies 2 keV, where the absorption is negligible, the photon loss is much smaller with XMM-Newton, compared to optical band. Therefore, XMM-Newton survey for clusters should be able to reach closer to the plane than traditional survey techniques. In this work we demonstrate the capability of detecting clusters behind the central regions of the Milky Way (see Nevalainen et al. [8] for the full analysis).

2 Observation

The XMM-Newton payload comprises 3 identical X-ray reflecting telescopes, the EPIC (European Photon Imaging Camera) imaging spectrometers, together with two reflection grating spectrometers and a co-aligned optical/UV monitor. The EPIC complement includes 2 conventional MOS CCD detectors (Turner et al. [11]) and a PN CCD instrument (Strüder et al. [10]). The former are placed behind the mirror systems containing grating arrays, the latter in the unobscured telescope. For more details of XMM-Newton see Jansen et al. [5]. In total the 3 EPICs provide >2500 cm^2 of collecting area at 1.5 keV. The mirror systems offer an on-axis full-width half maximum (FWHM) angular resolution of 4–5″ and a field of view (FOV) of 30′ diameter.

On 2000 April 11, during the calibration observation of a compact galactic supernova remnant G21.5-09, the source discussed here was discovered serendipitously. The new source is located on the opposite side of the FOV from G21.5-09 at an off-axis angle of 8′ at RA = $18^h\,32^m\,25.4^s$, dec. = $-10°\,36'\,45''$ (corresponding to galactic coordinates l = 21.3°, b = −0.7°) Exposures of 29 ks were taken with the 0.2–10 keV EPIC in full frame mode using medium thickness filters. The event lists produced by the XMM-Newton Science Analysis Software (SAS 5.0) tasks EMCHAIN and EPCHAIN were subsequently filtered using a third SAS task, XMMSELECT. For the MOS only X-ray events corresponding to patterns 0–12 were selected, while for the PN, only pattern 0 (single pixel) events were selected. Known hot, or flickering, pixels and electronic noise were rejected using the SAS.

We examined the effect of particle flares by extracting a light curve of all the CCDs in the >10 keV band. The light curve shows several short peaks, and a large flare towards the end of the observation. We rejected time bins using several different count rate criteria, ranging from no rejection at all to a very low level (0.4 count s^{-1} for the PN and 0.2 count s^{-1} for the MOS), which reduced the exposure time by 50%. Fitting the corresponding PN + MOS spectra revealed, that the fit parameters are virtually independent of the rejection level. However, to be safe, we chose to reject data obtained during the large flare close to the end, which reduced the exposure time to 26 ks.

3 Spatial Analysis

We used the SAS tool EEXPMAP to create exposure maps in the 1–10 keV energy range for the PN observation, and in 1–8 keV range for MOS1 and MOS2. The exposure maps include effects of the spatial dependence of the quantum efficiency, filter transmission and mirror vignetting. We used the images to derive radial surface brightness profiles for PN, and a combined one for MOS1 + MOS2 (Fig.1). Comparison of the surface brightness profile data with PSF shows that the source is clearly extended. With MOS data, we can detect the source out to a 2′ radius with 3σ confidence. A single β model provides a reasonable description of both PN and MOS data sets with $\beta = 0.53 \pm 0.02$ and $r_{\rm core} = 12'' \pm 1'' = 35 \pm 4\ h_{50}^{-1}$ kpc, The low value of the core radius is more suggestive of values obtained for rich cluster cooling flows than the larger scale ambient cluster emission.

In order to obtain information on the spatial distribution of the spectral properties of the cluster gas, we produced a color map, where color is defined as vignetting corrected PN counts in the 3–10 keV energy range, divided by the counts in the 1–3 keV energy ranges (Fig. 1). Within 1′ the color varies significantly, from 3 to 8. The emission in the South-West quadrant is soft (color ∼3), while the North-East quadrant is harder (color ∼3–5). Between them, aligned with the elongation axis of the total band brightness the emission is very hard (color ∼7–8).

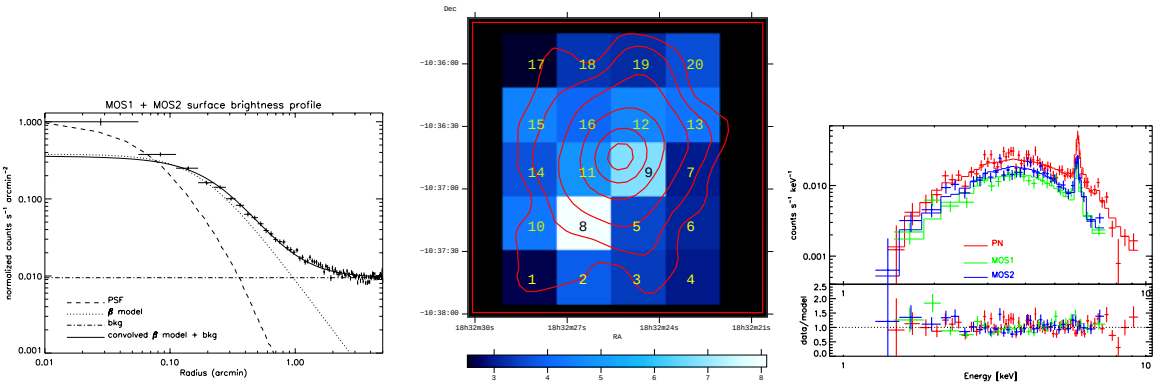

Figure 1: Left:The vignetting corrected MOS1 + MOS2 surface brightness profile in the 1–8 keV (crosses). The PSF (dashed line) is much narrower than the data, indicating that the source is extended. A best-fit β model to the $0.06' - 5'$ profile data (dotted line) convolved with the PSF + background (dot-dash), is shown as a solid line. Middle: The 3–10/1–3 keV color map obtained from PN data, overlaid with PN brightness contours. Right: The best-fit absorbed MEKAL model convolved with the instrumental responses of the PN, MOS-1 and MOS-2 are shown as solid lines, together with the data and 1σ uncertainties (crosses).

4 Spectral Analysis

We extracted the source counts from circular regions of $1'$ radius centered on XMMU J183225.4-10364 . For the background, we used the regions close to the source. As suggested by Saxton & Siddiqui [9], we used the ready-made on-axis energy redistribution matrices epn_fs20_sY9.rmf, M1_all.rmf and M2_all.rmf for the PN, MOS-1 and MOS-2, respectively, assuming that the response function does not vary significantly across the CCDs. We generated the vignetting corrected auxiliary response files with the SAS tool ARFGEN 1.41.12. In our fit, we excluded the strongly absorbed low energy band (below 1 keV), where most of the signal consists of redistributed photons from higher energies, and used the energy ranges 1–10 keV for the PN and 1–8 keV for the MOS. The net count rates in the above bands are 0.094 ± 0.002, 0.049 ± 0.002, and 0.060 ± 0.002 s^{-1} for the PN, MOS-1 and MOS-2, respectively.

We fitted the spectrum using the absorbed MEKAL collisionally ionized thermal plasma model in XSPEC v11.0.1. The N_H and the redshift were allowed to vary as well as the relative normalizations between the PN, MOS-1 and MOS-2 instruments. We obtained the best fit with parameters $N_H = (7.9 \pm 0.5)\ 10^{22}$ atom cm^{-2}, $T = 5.8 \pm 0.6$ keV, metal abundance of 0.60 ± 0.10 in Solar units and a redshift of $0.1242^{+0.0003}_{-0.0022}$ (see Fig.1 and Table 1). The fit is formally acceptable at a 90% confidence level with a χ^2 of 140.1 for 120 degrees of freedom (dof).

The redshift measurement depends critically on the centroid energy of the Fe K_α line, and thus on the accuracy of the instrument gain. We analyzed near-contemporaneous PN and MOS-1 data of revolution 59, (7 days before the observation of XMMU J183225.4-10364) of the internal in-flight calibration source at the location of the cluster using the same responses as for the source (MOS-2 data was not usable due to high background). We measured the line centroids to be within $\pm^{5}_{15}$ eV (or $\pm^{0.1}_{0.2}$ %) of the expected values. This implies a $\pm^{0.0002}_{0.0004}$ systematic component of the redshift determination, negligible compared to the statistical error of the redshift. Therefore our redshift measurement is robust.

5 Discussion

5.1 The nature of XMMU J183225.4-10364

At a redshift of 0.12, the spatial extent of $2'$ radius (see Sect. 3) corresponds to a physical diameter of 0.7 h_{50}^{-1} Mpc for the source. The only known bound objects on this scale are clusters

Table 1: The best fit values for XMMU J183225.4-10364 using WABS * MEKAL model in XSPEC. The uncertainties are given at 90% confidence level. The spectra are extracted within 1′ radius. The energy ranges used for the fits are 1–10 keV for PN and 1–8 keV for MOS-1 and MOS-2

param	value
T (keV)	5.8 ± 0.6
Metallicity (solar)	0.60 ± 0.10
$N_H(10^{22}$ atom cm$^{-2})$	7.9 ± 0.5
redshift	$0.1242 \pm {}^{0.0003}_{0.0022}$
χ^2/dof	140.1/120
F_{2-10} (10^{-12} erg s^{-1} cm^{-2})	$4.9 \pm {}^{1.0}_{0.6}$
L_{2-10} (h_{50}^{-2} 10^{44} erg s^{-1})	$3.5 \pm {}^{0.8}_{0.4}$

of galaxies and giant elliptical galaxies. The surface brightness profile of XMMU J183225.4-10364 is reasonably well described with 2 component β model, which is succesfully used to fit the ROSAT PSPC data of many cooling flow clusters. Our best fit values for the core radius and the slope are typical of the values in the above sample, supporting the cooling flow explanation.

Also, the source has a temperature of 6 keV, typical of rich clusters of galaxies. The iron abundance is somewhat higher than the typical cluster average, but at this redshift the 1′ extraction radius corresponds to 180 h_{50}^{-1} kpc, less than a typical cluster core radius. The recent study of a sample of BeppoSAX clusters (De Grandi & Molendi [2]) shows that in cooling flow clusters the metal abundances increase towards the center, reaching values consistent with ours. The spectral fit with a cooling flow model indicates a strong mass flow rate of $\sim 400 - 600$ $M_\odot$ yr^{-1}, consistent with values found for other clusters (e.g., White et al. [12]).

Within a 1′ circle centered at the brightness peak, we measure unabsorbed 2–10 keV fluxes and luminosities of $F_{2-10} = 4.9^{+1.0}_{-0.6} \times 10^{-12}$ erg s^{-1} cm^{-2}, and $L_{2-10} = 3.5^{+0.8}_{-0.4} \times h_{50}^{-2}$ 10^{44} erg s^{-1} and bolometric values of $F_{bol} = 1.0^{+0.2}_{-0.1} \times 10^{-11}$ erg s^{-1} cm^{-2}, $L_{bol} = 7.4^{+1.6}_{-0.9} \times h_{50}^{-2}$ 10^{44} erg s^{-1}. Extrapolating this flux with the two β model out to 1 Mpc sives $L_{0.1-2.4} = 1.5 \times h_{100}^{-2}$ 10^{44} erg s^{-1}, in agreement with L-T relation derived from ASCA cluster sample (Markevitch [7]).

5.2 Implications for Galactic plane Surveys

The ROSAT Position Sensitive Proportional Counter (PSPC) 8 ks observation of the G21.5-09 field (rp500126n00) shows no evidence for the presence of XMMU J183225.4-10364. This is consistent with the high absorption which strongly reduces the flux in the PSPC energy band. The 87 ks ASCA observation 50036000 of the G21.5-09 field reveals a weak source whose centroid is 3′ away from the cluster centroid determined from the PN image, probably consistent within the uncertainty envelopes. However, the source is too faint for any meaningful analysis. These facts indicate the power of XMM-Newton to enlarge our knowledge on the galaxy cluster distribution close to the Galactic plane.

De Grandi et al. [1] based on Rosat All Sky Survey data from the southern hemisphere provides an estimate of the density of clusters as a function of the ROSAT band flux. In this paper we have clearly demonstrated that at a 0.5–2.0 keV flux level of XMMU J183225.4-10364 within 1′ , ~ 3 10^{-12} erg cm^{-2} s^{-1}, is easily sufficient to measure redshifts accurately with XMM-Newton (for reasonable 10–30 ks exposures). De Grandi et al. (1999) then predict 60 such clusters per steradian. In XMM-Newton A0-1 there are about 10 square degrees of Galactic plane being covered in systematic surveys, which implies $\sim 20\%$ probablility of a detection. The above flux is similar to the limit in ROSAT Galactic plane cluster survey (Ebeling et al. [4]). Considering that the effective area of XMM-Newton exceeds that of ROSAT by a factor of 10, and that the

exposure times in the XMM-Newton surveys exceed those of RASS by a factor of 10, the actual minimum flux needed for XMM-Newton cluster detection, with reasonably accurate redshift measurement, will be 1-2 orders of magnitude lower than that of XMMU J183225.4-10364. This would increase the number of clusters detectable with XMM-Newton on the Galactic plane to between a few to tens per year assuming a similar sky coverage pattern to the currently scheduled observations.

In the Galactic plane galaxy redshifts are very difficult to measure using optical techniques due to the large amount of visual extinction and because of crowding. We have demonstrated here that XMM-Newton has the capability of measuring such redshifts, using the X-ray Fe K_α line. The systematic uncertainties induce ~ 10 eV uncertainty in the line centroid measurement which has a negligible effect compared to the statistical uncertainties in redshift measurements ($\sim 1\%$) for clusters with data of similar quality and with similar redshifts to XMMU J183225.4-10364. XMM-Newton data, over its projected 10 year lifetime will thus prove invaluable, in completing our picture of large scale structure in the local Universe and reducing the need for interpolation over a significan fraction of the sky.

Acknowledgments

Based on observations obtained with XMM-Newton, an ESA science mission with instruments and contributions directly funded by ESA member states and the USA (NASA). J. Nevalainen acknowledges an ESA Research Fellowship. We thank Dr F. Bocchino, Dr R. Jansen and Dr J. Kaastra for useful discussions.

References

1. De Grandi, S., Böhringer, H., Guzzo, L., et al. 1999, ApJ, 514. 148
2. De Grandi, S., & Molendi, S., 2001, ApJ, in press, astro-ph/0012232
3. Dickey, J., & Lockman, L. F., 1990, Ann. Rev. Ast. Astr. 28, 215.
4. Ebeling, H., Mullis, C., & Tully, B., 2000, astro-ph/0001319
5. Jansen, F., Lumb, D., Altieri, B., et al. 2001, A&A, 365, L1
6. Kraan-Korteweg, R. C., & Lahav, O., 2000, A&AAR, 10, 3, 211
7. Markevitch, M. 1998, ApJ, 504, 27
8. Nevalainen, J., Lumb, D., dos Santos, S., et al., 2001, A&, in press, astro-ph/0105131
9. Saxton, R. D., & Siddiqui, H. 2000, XMM-Newton technical note. XMM-PS-TN-43
10. Strüder, L. Briel, U., Dennerl, K., et al. 2001, A&A, 365, L18
11. Turner, M. J. L., Abbey, A., Arnaud, M., et al., 2001, A&A, 365, L27.
12. White, D. A., Fabian, A., C., Johnstone, R. M., et al. 1991, MNRAS, 252, 72